Effect of Ply Stacking Sequence on Stress in a Scarf Joint

Caryl L. Johnson*
Structural Dynamics Research Corporation, Inc., San Diego, California

Closed-form solutions for the stresses in an adhesive-bonded scarf joint indicate that the load is transferred over the entire overlap region. These solutions, however, do not consider the nonhomogeneity of laminated composites. This study investigates the effect of the stiffness discontinuity between individual plies and the variation of laminate stacking sequence on the joint's stress distribution. Highly detailed plane stress finite-element models of four- and twelve-layer scarf joints having alternating 0 and 90 deg plies were constructed. When subjected to a unit tensile load, these models produced stresses that were significantly different from the smooth curves predicted by closed-form solution. The different load-carrying capacity of the oriented plies caused irregular stress distributions whose characteristics were related to the location of each ply within the stack. Also, as the number of plies was increased, the stresses tended to oscillate within a limited band whose average was close to the results produced by an equivalent homogeneous laminate. Because the closed-form solution does not consider nonhomogeneous materials, this detailed analysis predicted trends in the stress distribution that otherwise could not be obtained.

Nomenclature

E_1	= Young's modulus of the isotropic adherend
E_{2x}, E_{2y}, E_{2z}	= Young's moduli of the composite adherend material
E_3	= Young's modulus of the adhesive
G_1	= shear modulus of the isotropic adherend
$G_{2xy}, G_{2xz}, G_{2yz}$	= shear moduli of the composite adherend material
G_3	= shear modulus of the adhesive
h_1, h_2	= thicknesses of the adherends
h_3	= thickness of the adhesive
$[K]$	= adhesive element stiffness matrix
$[\hat{K}]$	= transformed adhesive stiffness matrix
l	= adhesive element length
L_1, L_2	= extended length of the adherends beyond the overlap region
L_3	= joint overlap length = $h_{1/\tan}$
P_0	= applied tensile load
$[R]$	= transformation matrix
$SIG1X, SIG2X$	= X-direction stress in adherences 1 and 2
TAU	= adhesive shear stress along the scarf joint
u, v	= displacements of adhesive element nodes in local coordinates
x, y	= local adhesive coordinate system
X, Y	= global joint coordinate system
α	= scarf joint taper angle
ν_1	= Poisson's ratio of the isotropic adherend
$\nu_{2xy}, \nu_{2xz}, \nu_{2yz}$	= Poisson's ratios of the composite adherend material

Introduction

THE high-performance aircraft, spacecraft, and satellites developed by today's aerospace industry require extremely weight-efficient structures. This fact has resulted in the increasing use of laminated composite materials for both load-carrying primary and lightly loaded secondary components. However, since standard mechanical fastening techniques often produce inefficient load-transfer regions, other joining techniques must be employed.

Adhesive bonding is one technique that can produce highly efficient joints. The joints can be made in many different styles, each having its own advantages and disadvantages, as discussed by Hart-Smith.[1] In particular, the tapered scarf joint has been shown by Erdogan and Ratwani, using equilibrium equations, to produce an extremely efficient load transfer between two adherends.[2] Those authors found that if both adherends have equivalent stiffness, the stresses will be uniform along the joint. For unmatched adherends, the stresses will monotonically increase or decrease over the length of the overlap, but there will still be load transfer at all points along the joint. Numerical analyses performed later by Barker and Hatt also produced these same results.[3] In both studies, the adherends were assumed to be constructed from either isotropic or unidirectional laminated composites.

Advanced composite laminates constructed by stacking thin layers of material at various orientations are not homogeneous, and several studies have shown that the laminate stacking sequence can have a pronounced effect upon the internal stresses. For example, Pagano and Pipes found that the stacking sequence can significantly influence interlaminar shear stresses, and Rybicki and Schmueser determined that the stacking sequence will affect the stresses around a hole in a flat plate.[4,5] Therefore, the applicability of closed-form solutions and finite-element analyses having homogeneous material properties for representation of a nonhomogeneous laminate adherend should be investigated.

The study presented here was undertaken to determine whether the nonhomogeneity of advanced composite materials and variations in stacking sequence affect the stresses in an adhesive-bonded scarf joint. In particular, an attempt was made to produce specific stress distributions by placing longitudinal and transverse plies at different locations in the laminate, while maintaining the same thickness and effective stiffness. Detailed finite-element models were used to perform the analysis, with the closed-form equation providing a comparative solution for the equivalent homogeneous case.

Received March 31, 1987; revision received November 6, 1987.

*Project Engineer, Western Region Operations.

This paper first presents the scarf joint and finite-element model geometry and materials along with a brief description of the modeling assumptions employed. Then, results for two boron/epoxy adherend configurations, four and twelve layers, are presented and discussed. This is followed by a discussion of implications that these results may have on joint design practices and a final summary.

Scarf Joint Geometry and Materials

To allow for direct correlation between this study and the theoretical calculations performed by Erdogan and Ratwani, the scarf joint geometry, shown in Fig. 1, and the adherend materials were chosen to be identical to the ones used in their studies.[2] The materials are:

Adherend 1: isotropic aluminum

$$E_1 = 10^7 \text{ psi}$$
$$\nu_1 = 0.33$$
$$G_1 = 4.0 \times 10^6 \text{ psi}$$

Adherend 2: transversely isotropic boron/epoxy

$$E_{2x} = 32.4 \times 10^6 \text{ psi}$$
$$E_{2z} = E_{2y} = 3.5 \times 10^6 \text{ psi}$$
$$G_{2xz} = G_{2xy} = 1.23 \times 10^6 \text{ psi}$$
$$G_{2yz} = 1.35 \times 10^6 \text{ psi}$$
$$\nu_{2xz} = \nu_{2xy} = 0.23$$
$$\nu_{2yz} = 0.3$$

Epoxy adhesive

$$E_3 = 4.45 \times 10^5 \text{ psi}$$
$$G_3 = 1.65 \times 10^6 \text{ psi}$$

To select the specific joint geometry to be used, it is first necessary to define the goals of the study as they relate to typical joint applications. A characteristic of adhesive-bonded scarf joints is that, as the scarf angle increases, the shear strength of the adhesive, as compared to the adherends, becomes smaller. Eventually the adhesive strength becomes only a fraction of that of the adherends. To obtain maximum performance from a joint, normal design practice dictates that angles no greater than 2 deg be employed. On the other hand, to characterize adhesives using mechanical tests, the adhesive must be forced to fail before the adherends. Thus, scarf angles significantly greater than 2 deg are often employed in these cases. The goal of this study was to produce results that could be used in both practical and laboratory applications. Therefore, three different scarf angles of 2, 6, and 12 deg were considered, resulting in joints with the following constant geometric parameters:

$$h_1 = h_2 = 0.033 \text{ in.}$$
$$h_3 = 0.001 \text{ in.}$$
$$L_1 = L_2 = 0.384 \text{ in.}$$
$$L_3 = 1.587,\ 0.316,\ 0.956 \text{ in. for the 2, 6, and 12 deg joints, respectively}$$

In this case, an artifically low-adhesive thickness, 0.001 in., was selected to ensure that a worst-case scenario was considered. This low thickness will tend to accentuate the transferral of stress concentrations between the two adherends. Although somewhat unrealistic, this example does illustrate the effects of either using insufficient adhesive or omitting the adhesive altogether, which often occurs in practice.

Finite-Element Model

The analysis of the different stacking sequence variations used the standard static finite-element techniques provided by the program MSC/NASTRAN.[6] To obtain accurate results that could be compared to the closed-form solution, the following modeling guidelines were employed:

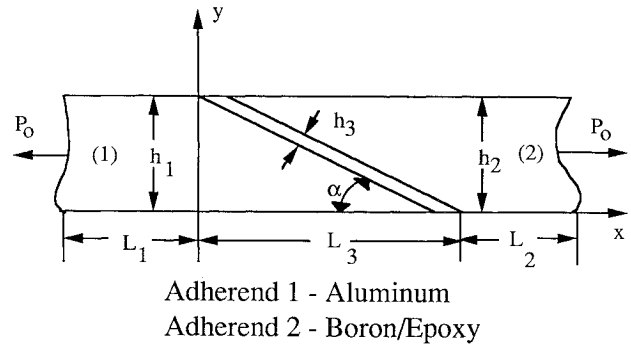

Fig. 1 Scarf joint geometry.

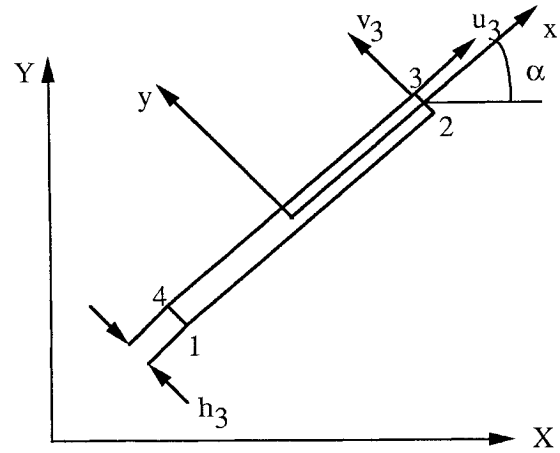

Fig. 2 Adhesive finite element.

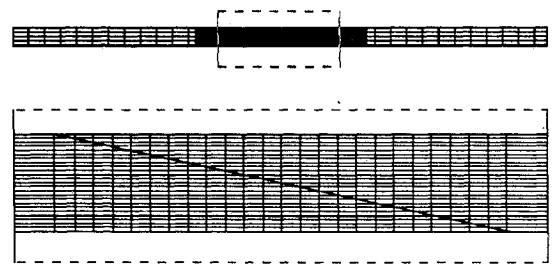

Fig. 3 Finite-element model, 12-deg joint.

1) Plane stress material and physical properties were used for all elements.

2) The models adhered to all dimensional assumptions employed by Erdogan and Ratwani[2] to ensure equivalent joint representations.

3) A minimum of two elements through the thickness of each ply was employed.

4) Linear quadrilateral or triangular elements were used to represent the adherends.

Representing the adhesive layer with quadrilateral elements would require aspect ratios that greatly exceed acceptable limits and would produce inaccurate results. In addition, attempting to use linear springs can cause stress singularity problems at the interface tips, as described by Bogy and Wang.[7] However, in their finite-element analysis of adhesive-bonded joints, Barker and Hatt found that both the numerical inaccuracy and singularity problems could be avoided by using a special adhesive element.[3]

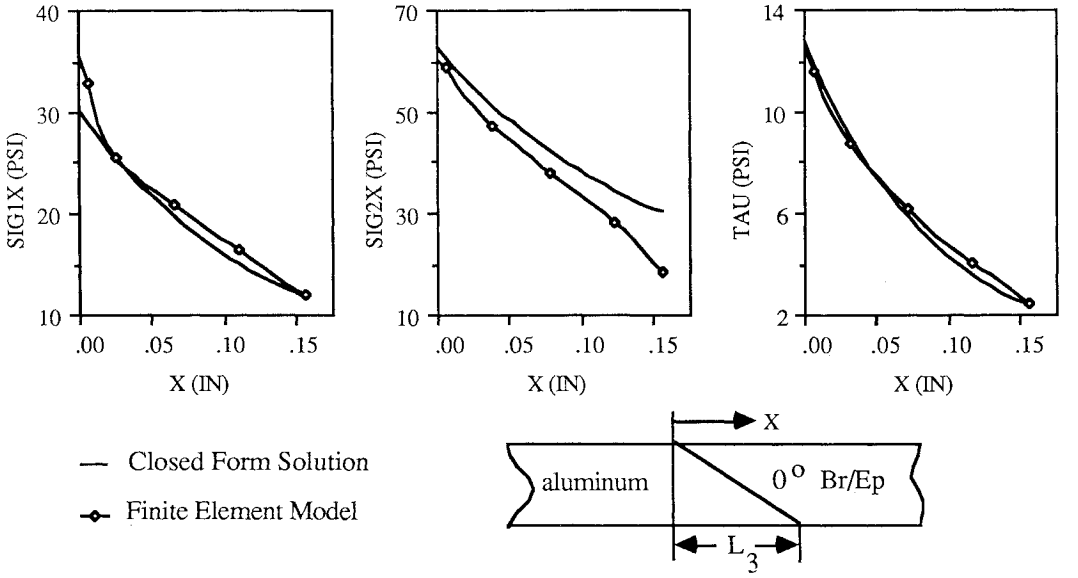

Fig. 4 Stress results for Al to 0 deg Br/Ep joint for $\alpha = 12$ deg.

This special adhesive element, shown in Fig. 2, assumes that the undisplaced nodes from one adherend (1 and 2) are coincident with the corresponding undisplaced nodes from the other (4 and 3), resulting in an element having zero thickness. The stiffness matrix itself then accounts for the thickness by including it in the derivation of each term. Originally derived by Goodman et al.,[8] the adhesive element stiffness matrix is

$$[K] = \frac{1}{6}\begin{bmatrix} 2k_s & 0 & k_s & 0 & -k_s & 0 & -2k_s & 0 \\ 0 & 2k_n & 0 & k_n & 0 & -k_n & 0 & -2k_n \\ k_s & 0 & 2k_s & 0 & -2k_s & 0 & -k_s & 0 \\ 0 & k_n & 0 & 2k_n & 0 & -2k_n & 0 & -k_n \\ k_s & 0 & -2k_s & 0 & 2k_s & 0 & k_s & 0 \\ 0 & -k_n & 0 & -2k_n & 0 & 2k_n & 0 & k_n \\ -2k_s & 0 & -k_s & 0 & k_s & 0 & 2k_s & 0 \\ 0 & -2k_n & 0 & -k_n & 0 & k_n & 0 & 2k_n \end{bmatrix}$$

where $k_s = G_3/h_3 l$ and $k_n = E_3/h_3 l$.

To orient the adhesive element properly when it is rotated by some angle α with respect to the global coordinate system, it is necessary to transform the stiffness matrix. The transformed matrix is obtained from

$$[\hat{K}] = \begin{bmatrix} R^T & & & \\ & R^T & & \\ & & R^T & \\ & & & R^T \end{bmatrix} [K] \begin{bmatrix} R & & & \\ & R & & \\ & & R & \\ & & & R \end{bmatrix}$$

where the transformation matrix $[R]$ is given by

$$[R] = \begin{bmatrix} \cos\alpha & \sin\alpha \\ -\sin\alpha & \cos\alpha \end{bmatrix}$$

This matrix, along with the proper nodal connectivity information, can be modeled in MSC/NASTRAN through the special GENEL general element.[6]

The modeling assumptions and the adhesive element were used to construct models for joints having three different scarf angles of 2, 6, and 12 deg. The 12 deg scarf model is shown in Fig. 3. A unit tensile load was imposed by restraining one end of the joint and applying a uniform displacement to all nodes on the opposite end. Finally, if left unrestrained, the joint would deflect from the bending moment caused by the mismatched stiffness of the two adherends. This in turn would produce results that differed significantly from those obtained from the closed-form solution. Barker and Hatt found that this could be prevented by restraining the nodes in the vertical direction along one edge.[3]

To validate the models, the finite-element results obtained for unidirectionl 0 and 90 deg laminated adherends were compared to the results obtained from the closed-form solution. The results for the 12 deg joint, shown in Figs. 4 and 5, indicate that in general the two analysis techniques produced closely matching results. The differences that appear could be due to the grid point stress extrapolation used to produce stresses along the joint edge. The results obtained for the 2 and 6 deg scarf joints were very similar to those for the 12 deg joint and are, therefore, not shown.

With the scarf joint finite-element models constructed and verified, it is possible to perform the study cases in which the material properties in each ply of the laminated adherend are individually varied.

Four-Layer Adherend Results and Discussion

The objective of the first group of laminate configurations was to determine whether the detailed analysis would produce results that were discernibly different from an equivalent closed-form solution and whether variations in the stacking sequence would affect these result. To achieve this objective, the laminated adherend was assumed to have only four layers of material – two at 0 deg and two at 90 deg – for a total of six possible configurations, as summarized in Table 1. Then, to provide a basis for comparison, the closed-form solution for an adherend having the homogeneous material properties of a 50% 0 deg and 50% 90 deg laminate was performed and its results presented with those from the finite-element analysis.

From the stress results for the 12 deg scarf angle (presented in Figs. 6-8) it is apparent that the distributions are greatly affected by the nonhomogeneity of the laminate. The smooth, monotonically decreasing curves that are predicted by Erdogan's theory are replaced by curves having a series of peaks and valleys with magnitudes that oscillate about the homogeneous solution. In all cases the maximum stress peak

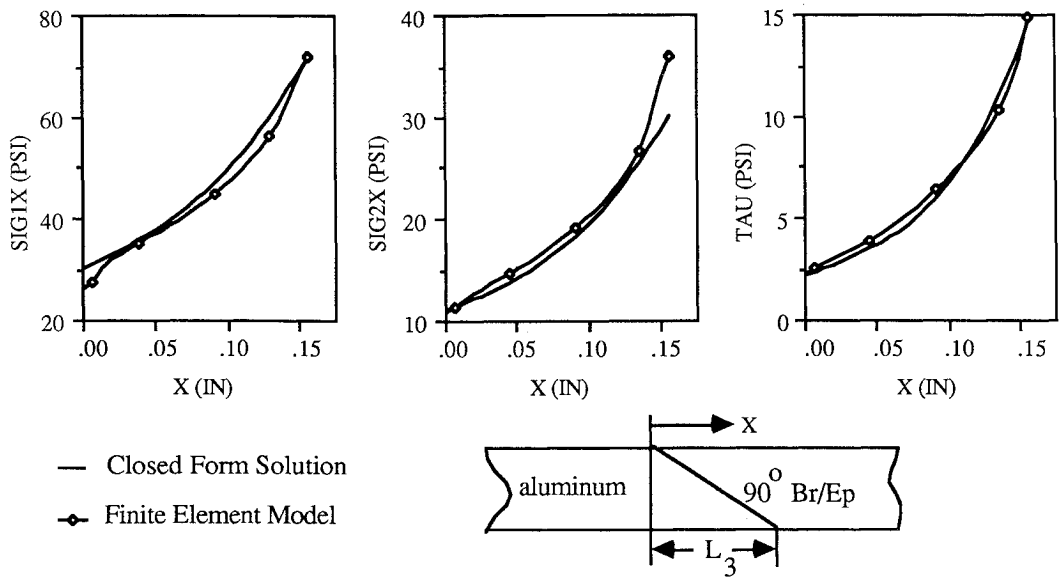

Fig. 5 Stress results for Al to 90 deg Br/Ep joint for $\alpha = 12$ deg.

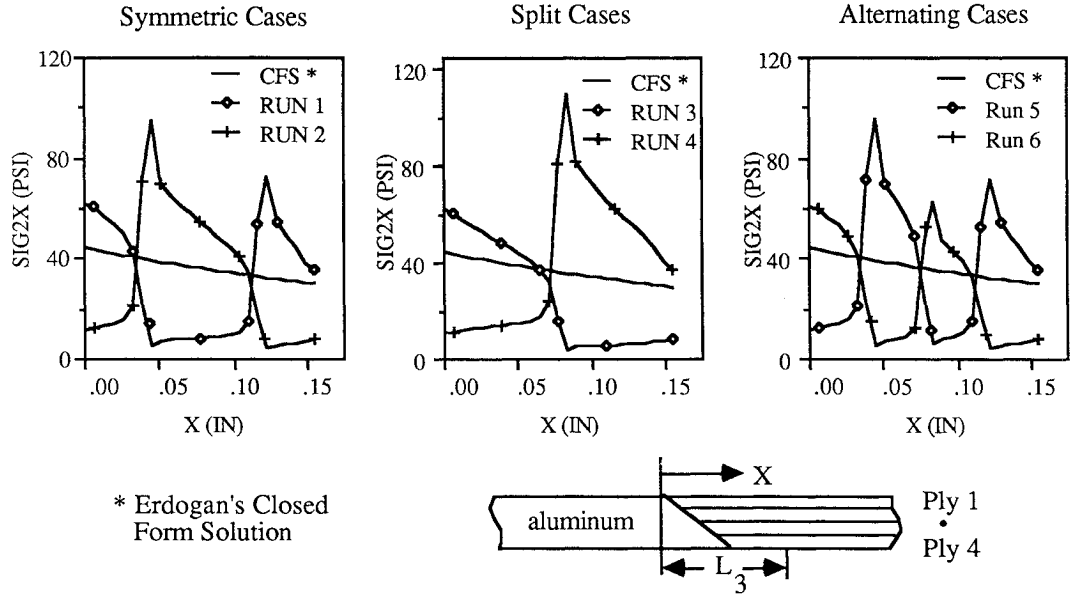

Fig. 6 X-direction stress in Br/Ep for $\alpha = 12$ deg.

is always equal to or greater than that predicted by the theory and occurs in locations that are entirely dependent on the location of the stiff 0 deg plies.

The boron/epoxy's longitudinal Young's modulus and, consequently, its interlaminar shear stiffness are approximately an order of magnitude greater than the matrix-dominated transverse properties. Thus, the 0 deg plies, having their stiffest properties aligned along the direction of the joint, carry significantly more load than the 90 deg piles. This produces highly critical interlaminer shear stresses between the plies, which is directly accountable for producing the large discontinuity in the logitudinal stresses indicated in Fig. 6. The aluminum, not containing any through-the-thickness changes in stiffness, would be expected to have a smooth stress distribution throughout. However, as shown in Fig. 7, it is evident that the irregular stress distribution in the boron/epoxy laminate is affecting the aluminum's stresses, although the degree of irregularity has been significantly diminished. Studying the adhesive shear stresses shown in Fig. 8, it is evident that its low modulus allows the adhesive to transfer the load over larger regions, effectively insulating the aluminum from the extreme stress peaks occurring in the boron/epoxy. Furthermore, in actual joints in which nonlinear material effects are produced, the plastic capabilities of the adhesive would even further alleviate these stress peaks. However, the extreme irregularity in the boron/epoxy would remain since resin matrices usually have very little plastic deformation capability.

Table 1 Stacking sequences for four-layer cases

Run id	Laminate stacking sequence
Run 1	$[0, 90]_s$
Run 2	$[90, 0]_s$
Run 3	$[0_2, 90_2]$
Run 4	$[90_2, 0_2]$
Run 5	[90, 0, 90, 0]
Run 6	[0, 90, 0, 90]

Comparing the laminated adherend stress distributions obtained from the different finite-element analyses (Fig. 6), it is

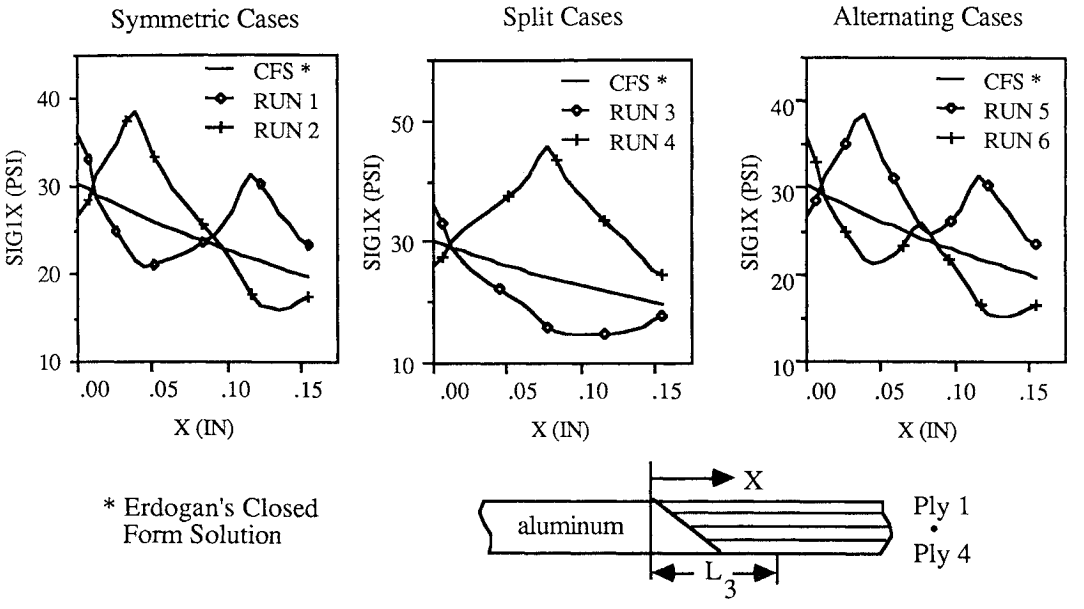

Fig. 7 *X*-direction stress in aluminum for $\alpha = 12$ deg.

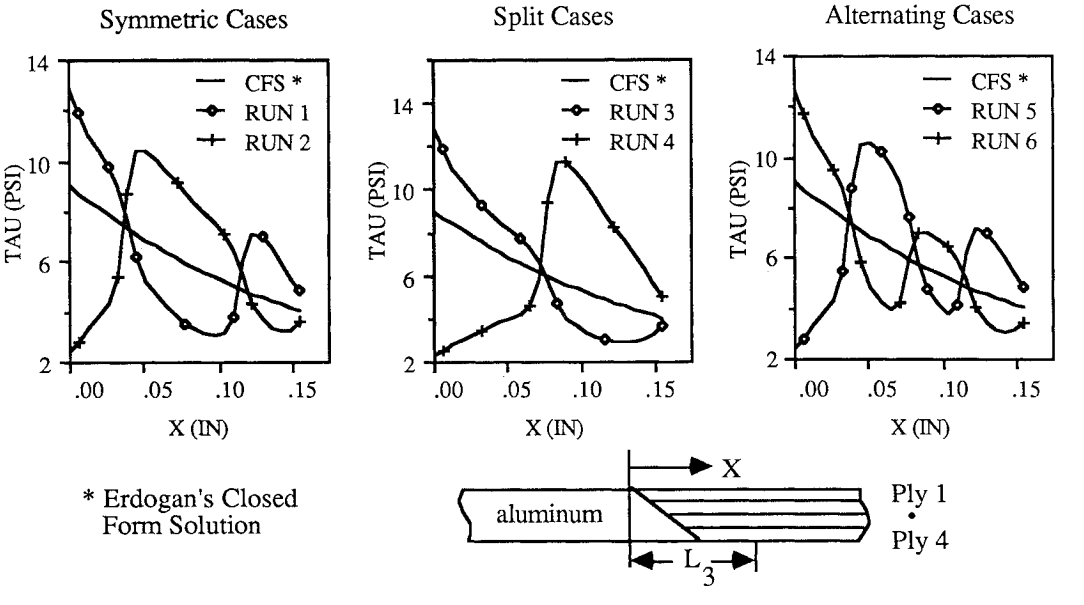

Fig. 8 Adhesive shear stress along joint interface for $\alpha = 12$ deg.

evident that the magnitude and location of the maximum peaks are directly related to the location of the 0 deg plies relative to the 90 deg plies. In general, the peaks are significantly larger in the cases where a 90 deg ply occurs at the start of the joint overlap, $x = 0$, than those where 0 deg ply is first. On the other hand, the aluminum adherend and adhesive stresses (Figs. 7 and 8) tend to have their highest stress peaks when the 0 deg plies are located first in the stack.

Finally, comparing the stress results for the 12 deg scarf angle with those obtained from the 2 and 6 deg scarf angles indicated that, with the exception of magnitude, the stress distribution trends as shown for the 12 deg scarf joint are valid for all three joint configurations. In general, the magnitude of the maximum stress peaks in the boron/epoxy adherend tends to increase as the scarf angle decreases, whereas the corresponding stress peak in the adhesive tends to decrease with decreasing angle, as shown in Fig. 9. The aluminum adherend stresses tend to remain the same for all angles. These results verify the original assertion that extremely small scarf joints, 1 to 2 deg, should be employed to create a practical design. Only then will the strength of the adherends be reduced to the point where they would fail before the adhesive.

Twelve-Layer Adherend Results and Discussion

The finite-element analyses completed for the four-ply cases indicated that the discontinuity in stiffness across each ply in a laminated adherend can have significant impact on the stresses in both the adherends and the adhesive. However, the construction of any laminated composite with such large concentrations of unidirectional plies is highly discouraged. In fact, this particular laminate would be entirely impractical, since the difference between autoclave and room temperatures would produce interlaminar shear stresses high enough to split the laminate between each 0 and 90 deg interface.

One goal of this study was to extend the results from the four-ply cases to a more realistic laminate. However, to obtain a practical laminate would require having at least 30 plies with

no more than two adjacent ones having the same orientation. At the time of this study, building and analyzing the large finite-element model capable of this representation was not feasible. On the other hand, it was possible to increase the number of plies to 12 with no modifications to the already created model. Even though this particular laminate is still impractical, it has provided an indication of how the stresses change as the number of plies increases. Thus, for this phase of the study, the laminated adherend was modified to represent 12 alternating layers of 0 and 90 deg plies divided into two asymmetric and two symmetric configurations, as defined in Table 2. As before, all results obtained for the twelve-layer analyses were compared to the same closed-form solution for the 50% 0 deg and 50% 90 deg laminate.

The stresses in the adherends and adhesive for the 12 deg scarf joint are plotted in Figs. 10–12. Because of the increased number of ply orientation transitions, the irregular stress distributions are significantly more erratic than those produced by the four-layer finite-element model. However, closer scrutiny shows that the magnitudes of both the maximum and minimum are restricted to lie within a limited band whose average is close to the results obtained for the equivalent homogeneous case. Whether this average is higher or lower than the homogeneous case is determined by whether a 0 or 90 deg ply is located first in the stacking sequence. From these results it can be deduced that continually increasing the number of plies decreases the width of the stress band and shifts the average value more toward the homogeneous solution. The limiting case would be the true homogeneous representation.

It is also evident from the symmetric cases that any grouping of plies having the same orientation, as found in the center of the joint, will produce noticeable effect upon the resulting joint stresses. In some instances, this effect manifests itself as a stress peak that has a larger magnitude than all surrounding peaks. In addition, it can be assumed that, as the number of unidirectional plies increases, the magnitude of this stress peak will also increase. Therefore, it is evident that the location and number of unidirectional plies used in the region of a scarf joint can significantly impact the integrity of the joint.

As in the four-layer cases, the irregular stress distributions were found to have the identical characteristics for all three scarf angles. Only the magnitudes of the maximum stresses were affected. In general, the stresses in the boron/epoxy adherend increase while the aluminum's stresses remained relatively unchanged, as shown in Fig. 13. The adhesive stresses, on the other hand, were significantly reduced as the scarf angle decreased, once again indicating that the smallest possible scarf angle should be selected to ensure a conservative joint design.

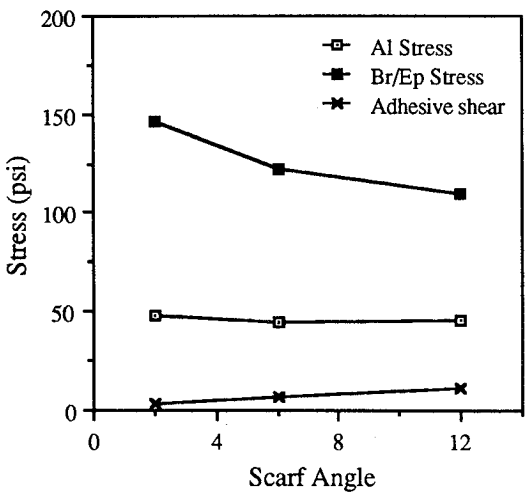

Fig. 9 Maximum stress vs scarf angle for the run 4 joints.

Summary and Recommendations

The results obtained from this finite-element analysis differed significantly from what is predicted by the closed-form solution, which does not consider the effects of nonhomogeneity. First, the smooth stress distributions that would be produced by the homogeneous analyses were not obtained for any of the cases considered. Instead, erratic curves were produced with large stress peaks whose magnitude and location were dependent on the location of the 0 and 90 deg plies. The magnitude of the maximum stresses was also dependent on the

Table 2 Stacking sequences for twelve-layer cases

Run id	Laminate stacking sequence
Run 7	$[(0, 90)_6]$
Run 8	$[(90, 0)_6]$
Run 9	$[(0, 90)_3]_s$
Run 10	$[(90, 0)_3]_s$

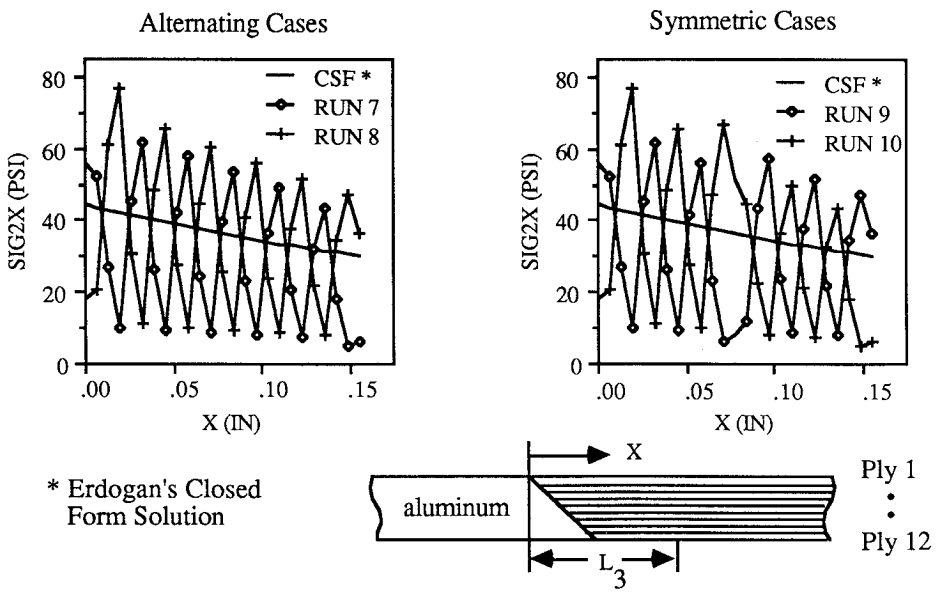

Fig. 10 X-direction stress in Br/Ep for $\alpha = 12$ deg.

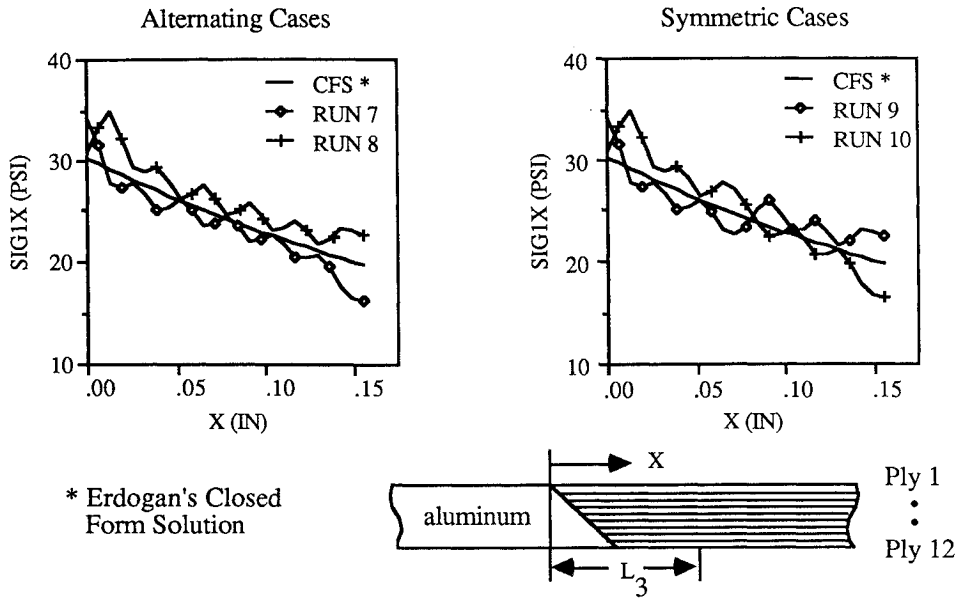

Fig. 11 *X*-direction stresses in aluminum for $\alpha = 12$ deg.

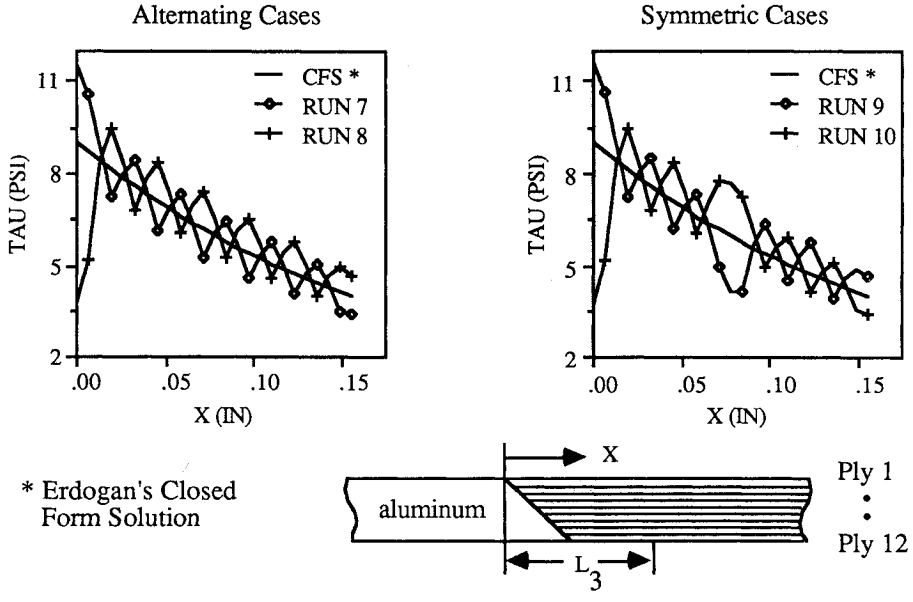

Fig. 12 Adhesive shear stress along the joint interface for $\alpha = 12$ deg.

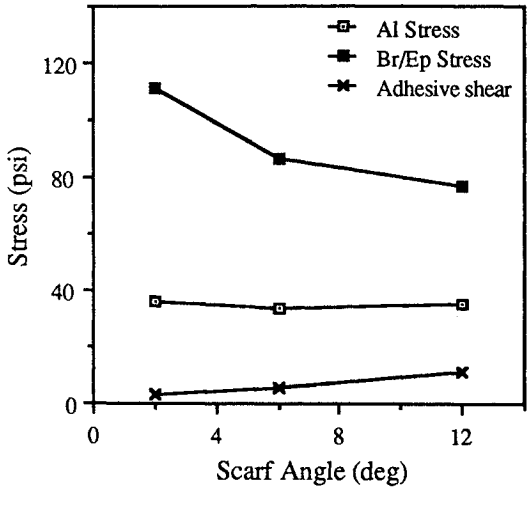

Fig. 13 Maximum stress vs scarf angle for the run 8 joints.

total number of alternating plies in the laminate and on the scarf joint taper angle. Finally, as the number of alternating plies increased, the stresses appeared to remain within a maximum and minimum boundary whose average is approximately equal to the homogeneous solution. Continuing to increase the number of plies decreases the width of this stress band until the exact homogeneous solution would be obtained in the limiting case.

Several important design considerations can be deduced from the results obtained in this study. Joining a laminated adherend with only a few plies or with only a few groups of plies having the same orientation produces excessively high stresses that cannot be predicted by the homogeneous theory. In particular, the homogeneous theory is unable to consider the interlaminar shear stresses that develop between discrete layers of material having different stiffnesses. In addition, since the homogeneous theories do not consider the effects of thermal stresses, joints that are analytically sufficient for the application, in fact, may not be manufacturable. Highly detailed ply-by-ply analyses are required to obtain an indication

of the true stresses in these types of joints. In general, to avoid any stress concentrations caused by the discrete plies, all laminated adherends should be constructed with as many alternating layers as possible. Then the homogeneous closed-form solutions along with generous factor of safety can be used to approximate the actual stress.

Finally, standard bonded joint design practices dictate that the adherends should be designed to fail before the adhesive. It is also essential that the most efficient joints be employed to maximize the weight benefits obtained from using laminated composite materials. For general adhesive-bonded scarf joints it is known that as the scarf angle increases the stresses in the adherends increase, and the shear strength of the adhesive decreases. With the additional stresses induced by large groups of unidirectional plies, it is obvious that the allowable strength of either the adherends or the adhesive could very quickly be reached. Thus, in addition to using many alternating layers in the laminated adherend, it is also highly recommended that the minimum possible scarf angle that does not cause adherend tip breakage be used.

Conclusion

This study has provided some additional insight into the behavior of a bonded scarf joint between an isotropic adherend and a laminated adherend. An extremely detailed finite-element representation of a typical joint subjected to a unit tensile load has revealed that the closed-form solutions used to determine the strength of a scarf joint produced nonconservative stress results when the laminated adherend is highly nonhomogeneous. It has also shown that severe stress peaks, whose magnitudes and locations depend on the location of the stiffest plies, may occur in both adherends and the adhesive. Thus, it is essential that the designer and analyst fully understand the impact of these stress peaks on the overall strength of the joint.

References

[1]Hart-Smith, L. J., "Adhesive-Bonded Joints for Composites – Phenomenological Considerations," Technology Conferences Associates Conference on Advanced Composites Technology, El Segundo, CA, March 1978.

[2]Erdogan, F. and Ratwani, M., "Stress Distribution in Bonded Joints," *Journal of Composite Materials*, Vol. 5, July 1971, pp. 378–393.

[3]Barker, R. M. and Hatt, R. B., "Analysis of Bonded Joints in Vehicular Structures," *AIAA Journal*, Vol. 11, Dec. 1973, pp. 1650–1654.

[4]Pagano, N. J. and Pipes, R. B., "The Influence of Stacking Sequence on Laminate Strength," *Journal of Composite Materials*, Vol. 5, July 1971, pp. 55.

[5]Rybicki, E. F. and Schmueser, D. W., "Effect of Stacking Sequence and Layup Angle on the Free Edge Stresses in a Hole in Laminated Plate Under Tension," *Journal of Composite Materials*, Vol. 12, July 1978, pp. 300.

[6]McMcormick, C. W. (ed.), *MSC/NASTRAN User's Manual*, Vol. 1, MacNeal-Schwendler Corp., Los Angeles, CA, 1985.

[7]Bogy, D. B. and Wang, K. C., "Stress Singularities at Interface Corners in Bonded Dissimilar Isotropic Elastic Materials," *International Journal of Solids and Structures*, Vol. 7, Aug. 1971, pp. 993–1005.

[8]Goodman, R. E., Taylor, R. L., and Brekke, T. L., "A Model for the Mechanics of Jointed Rock," *Journal of the Soil Mechanics and Foundations Division; Proceedings of the American Society of Civil Engineers*, Vol. 3, American Society of Civil Engineers, New York, May 1968, pp. 637–659.